Arabian Journal of Chemistry (2023) **16**, 104871

King Saud University

Arabian Journal of Chemistry

www.ksu.edu.sa
www.sciencedirect.com

ORIGINAL ARTICLE

Slow release fertilizers based on polyphosphate/montmorillonite nanocomposites for improving crop yield

Guiting Yang [a], Hongmeng Zhao [b], Yanli Liu [c], Zeli Li [c], Feng Gao [c], Qiang Zhang [d], Peng Zou [d], Zhiguang Liu [c,e,*], Min Zhang [c,*]

[a] *Institute of Agricultural Resources and Environment, Jiangsu Academy of Agricultural Sciences, Nanjing 210014, China*
[b] *State Key Laboratory of Soil and Sustainable Agriculture, Key Laboratory of Soil Environment and Pollution Remediation, Institute of Soil Science, Chinese Academy of Sciences, Nanjing 210008, China*
[c] *National Engineering Research Center for Efficient Utilization of Soil and Fertilizer Resources, Shandong Agricultural University, Taian 271018, China*
[d] *State Key Laboratory for the Integrated Use of Nutritional Resources, Kingenta Ecological Engineering Group Ltd., Linshu, Shandong 276700, China*
[e] *Shandong Wanhao Fertilizer Co. Ltd., Jinan 251600, China*

Received 30 January 2023; accepted 24 March 2023
Available online 30 March 2023

KEYWORDS

Nanocomposite fertilizers;
Particle strength;
Spherical;
Montmorillonite;
Polyphosphate

Abstract Nanocomposites are promising materials for the development of novel and environmentally friendly fertilizers that can delay the release of nutrients. In this study, a novel high-strength spherical nanocomposite fertilizer was prepared via agglomeration and granulation using montmorillonite, urea phosphate, urea, and potassium chloride as raw materials. The properties and morphology of the prepared fertilizer were characterized by Fourier Transform Tnfrared Spectroscopy (FT-IR), X-ray Diffraction (XRD), Scanning Electron Microscope (SEM), Transmission Electron Microscope (TEM), Thermogravimetric Analysis (TGA) and X-ray Computed Tomography (XCT) techniques. FT-IR analysis identified the formation of polyphosphate in fertilizer and hydrogen bonds between polyphosphate and montmorillonite. XRD analysis showed increased montmorillonite interlayer spacing and confirmed the formation of polyphosphate-montmorillonite nanocomposites. The effects of raw material mass ratio, reaction time, and reaction temperature on the strength and fluidity of nanocomposite fertilizer granules and the optimum preparation process was obtained by the response surface method (RSM-CCD). The optimum preparation process

* Corresponding authors.
E-mail addresses: liuzhiguang8235126@126.com (Z. Liu), minzhang-2002@163.com (M. Zhang).
Peer review under responsibility of King Saud University.

Production and hosting by Elsevier

https://doi.org/10.1016/j.arabjc.2023.104871

was obtained as follows: reaction temperature, 103 °C; reaction time, 237 min; and mass ratio, 1:1:0.93:1 (urea phosphate: urea: potassium chloride: montmorillonite). Under these optimum conditions, the particle hardness and angle of repose of the prepared fertilizer were 64.75 ± 0.48 N and 30.84 ± 0.95°. Nutrient release and agronomic effectiveness of the fertilizer was evaluated using column leaching and pot experiments, respectively. The column leaching experiment and XCT analysis demonstrated that the nanocomposite structure was responsible for the slow nutrient release. The pot experiment showed that compared with the traditional fertilizer, the soil nitrate and available phosphorus was increased by 28.02% and 43.45%, respectively, and the maize yield was increased by 24.27% with the application of prepared fertilizer. This work provides support for the preparation of high-strength spherical nanocomposite fertilizers and their large-scale applications in modern mechanical agriculture.

1. Introduction

Chemical fertilizers play an irreplaceable role in agricultural production and increase crop yield (Xin et al., 2017; Yahaya Et Al., 2022). However, the agronomic efficiency of traditional fertilizers is generally low, with high nutrient losses (50% on average) to the soil, water, and environment, which can trigger serious environmental problems (Ren et al., 2022). Hybrid nanomaterials have recently received extensive scientific interest owing to their slow-release properties, which can be used for slow-release fertilizer production (Guha, et al., 2020). Nutrients diffuse slowly through the obstacle in the nanocomposite structure, volatilization and leaching of nutrients are reduced, and fertilizer utilization efficiency is improved (Kim et al., 2011; Wang et al., 2014; An et al., 2017; Pereira et al., 2017).

Montmorillonite is a type of low cost and eco-friendly natural nano clay material with an alumina octahedral sheet between two silica tetrahedral sheets in its layered structure (Zhou et al., 2017; Sandomierski et al., 2020). Montmorillonite has been widely used to prepare sustained-release nanocomposites because of its nanoparticle size, large specific surface area, special nano-interlayer domain and strong cation-exchange ability (Setshedi et al., 2013; Dziadkowiec et al., 2017; Zhu et al., 2019). Nutrient elements are commonly dispersed into the clay matrix of nanocomposites by using mechanical methods such as extrusion, ultrasound, dipping, and grinding (Golbashy et al., 2017; Madusanka et al., 2017; Borges et al., 2018; Jahangirian et al., 2020; Zhang et al., 2020). The lamellar structure of montmorillonite inhibits the diffusion of nutrients from the interlayer domain to the exterior. Golbashy et al. prepared a powdered montmorillonite-urea nanocomposite material for slow-release nitrogen fertilizer using a water suspension technique (Golbashy et al., 2017). Pereira et al. prepared a cylindrical urea/montmorillonite slow-release nanocomposite material by intercalating urea into montmorillonite using an extrusion process at room temperature (Pereira et al., 2012). Table S1 demonstrate the comparison of recent advancements in nanocarrier as fertilizer for slow nutrient release. Based on our literature investigation, nanocomposite fertilizers generally contain only one or two nutrient elements. In addition, they are usually cylindrical particles or powder at present, which makes it difficult to mix them with other fertilizers for application. Their properties such as low mechanical strength and poor flowability are unfavorable for mechanized fertilization. Moreover, nanocomposite fertilizer particles break up readily and produce dust during transportation and application, resulting in economic loss and posing potential risks to human health and the environment (Yamamoto et al., 2016; Kabiri et al., 2020).

Agglomeration granulation is the preparation of particles preparation from powdery materials using binders under the continuous rotation of a granulator (drum or disc) (Degrève et al., 2006; Mathur et al., 2016). In the granulation process, the powdery materials mainly undergoes three main stages: the wetting nucleation, collision growth, and crushing wear stages (Chai et al., 2017; De Simone et al., 2018; Obraniak et al., 2019; Heidari et al., 2020). Agglomeration granulation is widely used because it is simple, inexpensive, and hasa a high granulation rate (Washino et al., 2013; Albadarin et al., 2017). In addition to the shape, the strength of fertilizer particles is also an important index for evaluating their suitability for mechanical fertilization (Subero-Couroyer et al., 2005, Guo et al., 2018; Kabiri et al., 2018). Fertilizer particles with low mechanical strength break up during transportation, storage, and fertilization. Ammonium polyphosphate is a polymer with high nitrogen and phosphorus contents (Lim et al., 2016). It is usually used as a fire extinguishing agent at high degree of polymerization (>20) and as a fertilizer with a low degree of polymerization (Yang et al., 2019, Asimakopoulou et al., 2020). Polyphosphate can be formed by heating urea phosphate and urea (Lewis et al., 1983, Hodge and Motes 1994, Cichy and Folek, 2005). In this study, a spherical granular fertilizer was prepared by agglomeration and granulation using urea phosphate and urea as raw materials, and ammonium polyphosphate with a low degree of polymerization was formed via a heating reaction. The ammonium polyphosphate chains cross each other, improving the adhesion between the internal particles and increasing the particle strength of the fertilizer. Additionally, montmorillonite's unique "sandwich" structure can be exfoliated into graphene-like nanosheets, which are uniformly dispersed and interlocked with ammonium polyphosphite molecular chains to enhance the mechanical properties of nanocomposites (Zhu et al., 2019, Bhat et al., 2022, Idumah et al., 2022). However, the reaction between urea phosphate and urea can cause deformation of the fertilizer particles, which can negatively affect their efficiency and application. Therefore, in this study, we introduced potassium chloride into the formulation to alleviate this issue. Potassium ions were adsorbed by the negative charges of adjacent layers, and the strong interlayer binding also suppressed the interlayer changes of montmorillonite and resolving the problem of fertilizer deformation caused by high-temperature liquefaction during the reaction between urea phosphate and urea (Yang et al., 2017, Ren et al., 2021).

In the study, a novel high-strength nanocomposite slow release fertilizer was prepared by using urea phosphate, urea, potassium chloride, and montmorillonite as raw materials through the process of agglomeration granulation followed by heating. The objectives of the research were (1) to prepare a high-strength spherical nanocomposite slow-release fertilizer and to characterize its physicochemical properties and morphology using SEM, FTIR, XRD and other analytical techniques; (2) to optimize the process parameters using response surface methodology (RSM-CCD) to obtain the optimal reaction conditions and material ratios; and (3) to evaluate the nutrient release rate and agronomic effects of the prepared fertilizer through leaching column and maize pot experiments. This study provides a new method for preparing montmorillonite-based nanocomposite fertilizers that are environmentally friendly and suitable for use in mechanical agriculture.

2. Materials and methods

2.1. Materials and reagents

Urea ($CO(NH_2)_2$, >99%) was supplied from Luxi Chemical Co., Ltd. (Shandong, China), potassium chloride powder (KCl, >98%) was purchased from Qinghai Salt Lake Potash Fertilizer Co., Ltd. (Qinghai, China), montmorillonite (>96%) was purchased from Lingshou County Ruixin Mineral Powder Factory (Hebei, China), and phosphoric acid (H_3PO_4, >85%) was purchased from Kaitong Chemical Industry Co., Ltd. (Tianjin China).

2.2. Fertilizer preparation

2.2.1. Urea phosphate preparation

In a 500-mL round bottom flask, 236.13 g phosphoric acid was added to react with 150 g urea at 80 °C for 40 min while stirring. Then the mixture was poured into a 500-mL beaker and placed in an incubator to crystallize at 20 °C for 24 h. Finally, the mixture was filtered, and urea phosphate was obtained.

2.2.2. Fertilizers preparation via granulation

Urea phosphate, urea, potassium chloride, and montmorillonite were weighed, ground, sieved (60 mesh), mixed thoroughly, and poured into a homemade disc granulator [29]. Subsequently, water (3% by weight) was sprayed slowly on the powdery material using a small atomizer at a constant speed to avoid the falling loss of the powdery material. The agglomerated granules were screened to obtain 3–5 mm fertilizer particles, which were heated in the oven at an interval of 10 °C between 30 °C and 140 °C, and 100 min was heated at each temperature node. To investigate the effect of the material ratio on the strength and fluidity of the fertilizer particles, nanocomposite fertilizers were prepared with various ratios of raw materials (Table 1).

2.3. Characterization of the prepared fertilizers

The prepared fertilizers were characterized using an infrared absorption spectrometer (Nicolet IS 10, USA). The solid samples were ground into powder, pressed into KBr pellets, and scanned in the range of 400–4000 cm^{-1}. The morphologies of the different fertilizers were observed using scanning electron microscopy (SEM, SU8080, Hitachi Ltd., Japan) and a transmission electron microscope (TEM, JEM 2100F, JEOL Ltd., Japan). X-ray diffraction (XRD) analysis of the composites was performed using a Shimadzu XRD 6000 diffractometer (Bruker D8 Advance, Germany). The relative intensity was registered in a diffraction range (2θ) of 3–10°, using a Cu Kα incident beam (λ = 0.1546 nm). The scanning speed was 1° min^{-1} and the voltage and current of the X-ray tube were 30 kV and 30 mA, respectively. Diffraction patterns were analyzed using JADE 6.0. The prepared fertilizer was analyzed by thermogravimetric analysis (TGA, TGA/DSC 3+, Mettler Ettler Toledo, Switzerland) under air flow condition with ramping rate of 10 °C min^{-1}. Surface areas were calculated using the BET equation. The surface-area (BET) and pore size (Dp) measurements of samples were done on gas adsorption instrument (ASAP 2460, Micromeritics, America) at 77 K.

The 3D internal microstructures of UM, UPUKM, and UPUKM after elution were observed using 3D X-ray Computed Tomography. Tomographic scans were performed using a synchrotron beamline for full-field microtomographic imaging. Samples were analyzed with a Nanotom S (Phoenix, Ltd., Germany), using a 100 kV 100 μA X-ray source, with a final image resolution of 2 μm/pixel. A filtered back-projection-based reconstruction software was used to reconstruct cross-sectional images from microtomographic projections to 3D images.

Table 1 Nanocomposite fertilizers prepared with the raw materials at different mass ratios and their nomenclatures. The raw materials used were montmorillonite (M), urea (U), potassium chloride (K), and urea phosphate (UP).

Nomenclature	UP: U: K: M by mass
UM	0:1:0:1
UPM	1:0:0:1
KM	0:0:1:1
UPU	1:1:0:0
UPUM	1:1:0:1
UPUKM	1:1:1:1

2.4. Particle strength determination

Particle strength or particle hardness was a measure of the resistance of granules to deformation or fracture under pressure. For the measurement of particle hardness, fertilizer samples were first screened with a standard sieve to obtain granules with a size of 3.50–4.50 mm. Then, the particle hardness was measured for hardness by applying an increasing compressive force on a single particle with a particle hardness tester (Yinhe Instrument Factory, Jiangyan, China). The load at which 20 granules of a fertilizer fractured was averaged and reported as the particle hardness (N) of the fertilizer.

2.5. Particle fluidity determination

The angle of repose is the slope measured at the base of a pile of uncompressed granular solids when runoff occurs (Dubey and Mailapalli 2019; Ferreira et al., 2021). It is an indicator of particle fluidity and roundness. A larger angle of repose indicates lower particle fluidity, and a smaller angle of repose indicates higher particle fluidity (Tian et al., 2019). A fertilizer sample of 100 mL was placed into the funnel of an angle of repose tester (FBS104, FURBS, China), and the accumulation height (h) of the fertilizer was measured. Angle of repose (ϕ) was calculated according to Eq. (1).

$$\phi = \frac{\left(\arctan\left(\frac{h}{5}\right)\right)180}{\pi} \quad (1)$$

2.6. Optimization of UPUKM preparation by response surface methodology (RSM)

Response surface methodology is a good mathematical statistical method for process improvement and optimization with a small number of experiments (Danmaliki et al., 2017; Chelladurai et al., 2021). To investigate the effects of the raw

material ratio, reaction temperature, and reaction time on the properties of the prepared UPUKM, a center composite design (CCD), a standard RSM design, was adopted for model development by using the Design-Expert V11.1.0 software.

According to the previous experimental results (Fig. 1), the reaction of urea phosphate and urea will change the shape of fertilizer particles, so it is necessary to choose lower reaction temperature and longer reaction time. First, the optimum mass of urea phosphate (A) and potassium chloride (B) was evaluated under the reaction temperature of 90 °C and reaction time of 300 min. In order to obtain the fertilizer with more balanced nutrient elements, both the amounts of urea and montmorillonite were 1, and the masses of urea phosphate (A) and potassium chloride (B) were set to 0.5 and 1. The parameter range values in Table 2 are obtained by inputting the parameters into the design-expert V11.1.0 software. The masses of urea phosphate (A) and potassium chloride (B) were selected as independent variables (Table 2), and the fluidity and strength of fertilizer particles were taken as response parameters, with the matrix design shown in Table S2. In order to obtain the more energy-saving fertilizer preparation conditions, the reaction temperature was set to 80 °C and 120 ℃, and the reaction time was set to 120 min and 300 min, according to the previous experimental results (Fig. 1). The effects of reaction temperature (C) and time (D) on the fluidity and strength of fertilizer particles were analyzed using a 2^2 full factorial design (Tables 3 and S2). Finally, the results from the two RSM-CCD designs were combined to obtain the optimum process conditions for UPUKM preparation.

2.7. Evaluation of the nutrient release behavior of the prepared fertilizers

The nutrient release behavior of the prepared fertilizers was evaluated using a column leaching experiment. Rigid polyvinyl chloride columns with an inner diameter of 4 cm and a height of 30 cm were used. The columns were packed with a bottom layer of 15 cm quartz sand; a middle layer, which was the fertilizer sample; and an upper layer of 5 cm quartz sand (Fig. S1). Three grams of UPUKM and 2.25 g of conventional chemical fertilizer (CCF) were used so that the columns had the same nutrient contents. The CCF was a mixture of urea phosphate, urea, and potassium chloride. Filter papers were placed on top of the upper quartz sand layers to minimize surface erosion during rain simulation. A nylon mesh (80 mesh) was placed at the bottom of each column to prevent sand loss during the experiments. First, 76 mL water was added to saturate the column. Next, 408 mL more water was added. The amount of water used was based on the average seasonal rainfall in Taian City, Shandong Province (469 mm, National Meteorological Center of China, https://en.weather.com.cn/) and the cross-sectional area of the leaching column. The water flow rate was set to 34 mL h^{-1} using a peristaltic pump

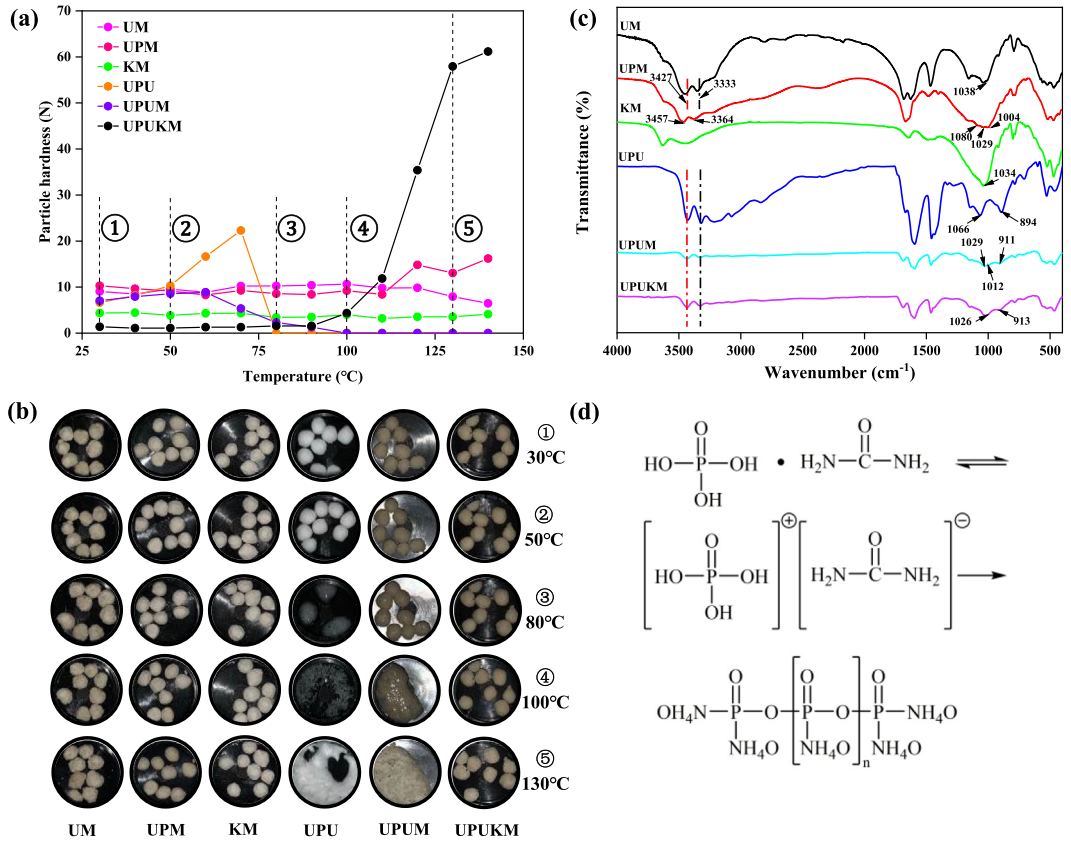

Fig. 1 Particle hardness (a) and images (b) of the prepared fertilizers at different temperatures, FTIR spectra of fertilizer after preparation (c), and scheme for generation of polyphosphate via the polycondensation reaction between urea phosphate and urea (d). See Table 1 for details of the fertilizers.

Table 2 Independent variable values of the fertilizer preparation process and their corresponding levels.

Independent variable	Level				
	−1.1472	−1	0	1	+1.1472
Urea phosphate	0.4	0.5	0.75	1	1.1
Potassium chloride	0.4	0.5	0.75	1	1.1

Table 3 Independent variable values of the fertilizer preparation process and their corresponding levels.

Independent variable	Level				
	−1.1472	−1	0	1	+1.1472
Reaction time (min)	83	120	210	300	337
Reaction temperature (°C)	72	80	100	120	128

(LabN1, Baoding Shenchen Pump Co., Ltd.), and the leachate was collected for analysis of nitrogen, phosphorus, and potassium analysis. Nitrogen was quantified using the Kjeldahl method. Total phosphorus content was determined using potassium persulfate digestion-molybdenum spectrophotometry. Total potassium was measured by flame emission spectrophotometry.

2.8. Evaluation of fertilizer agronomic effectiveness

A pot experiment was conducted at the New Fertilizer Experimental Station of Shandong Agricultural University in Tai'an, Shandong Province, China (117°13′ E, 36°20′ N), from June to September 2019. The soil used was collected from Binzhou City, Shandong Province (117°92′ E, 37°90′ N). This coastal salinized fluvo-aquic soil is classified as a Parasalic Ochri-Aquic Cambosol according to Chinese soil taxonomy. The basic physical and chemical properties of the soil were as follows: organic matter 7.69 g kg^{-1}, total nitrogen 0.50 g kg^{-1}, total phosphorus 1.83 g kg^{-1}, total potassium 35.94 g kg^{-1}, available nitrogen 85.58 mg kg^{-1}, available phosphorus 13.95 mg kg^{-1}, available potassium 186.19 mg kg^{-1}, pH 8.72, and total salt content 0.21%. Pottery pots (30 cm in diameter and 36 cm in height) were used and maize (*Zea mays* L. cv. Zhengdan 958) were grown with one maize plant per pot. Three treatments were set up with four replicates: CK (without fertilizer), CCF (conventional chemical fertilizer with N-P_2O_5-K_2O of 21–14-20), and UPUKM (14–11-16). The CCF was composed of urea, diammonium phosphate, and potassium chloride. For the CCF and UPUKM treatments, each pot received 5.40 g N, 1.44 g P_2O_5, and 3.60 g K_2O at the beginning of the experiment.

At the jointing stage of maize, soil samples were collected from each pot for nutrient analysis. Soil NO_3^--N and NH_4^+-N were extracted with 0.01 mol L^{-1} $CaCl_2$ (soil-solution ratio of 1:10) and determined with a continuous flow injection analyzer (AA3, Bran. Luebbe, Germany). Soil available potassium was extracted with 1 mol L^{-1} ammonium acetate and quantified with a flame photometer. Soil available phosphorus was extracted with 0.5 mol L^{-1} sodium bicarbonate and determined with an automatic discontinuous chemical analyzer (Smartchem200, USA).

2.9. Statistical analysis

All data were subjected to analysis of variance (ANOVA) using SPSS software (SPSS 22, USA) followed by a mean comparison using Duncan's multiple range test ($p < 0.05$).

3. Results and discussion

3.1. Preparation of fertilizer based on polyphosphate/montmorillonite nanocomposites

The particle shape of UM, UPM, KM and UPUKM was remained spherical at 30–140 °C, while the particle strength of fertilizer in UM, UPM and KM did not change significantly, and the particle strength was low (Fig. 1a, b). In UPUKM, the particle strength of the fertilizer gradually increased, reaching 63.2 N at 140 °C. The FTIR analysis showed that the peak at 913 cm^{-1} in UPUKM was the tensile vibration absorption peak of P-O-P (Fig. 1c), indicating a polycondensation reaction occurred between urea phosphate and urea and polyphosphate was generated (Fig. 1d) (Gong, 2001; Wang et al., 2017; Naraginti et al., 2019), while no such peak was found in UM, UPM and KM. This also shows that the formation of polyphosphates increases the particle strength of fertilizers. The particle strength of fertilizer can be increased by forming polymer. Yamamoto et al. prepared a kind of urea/urea–formaldehyde/montmorillonite nanocomposite by extrusion and granulation and heating, which increased the mechanical strength of fertilizer based on urea/montmorillonite nanocomposite (Yamamoto et al., 2016). However, the fertilizer prepared by extrusion was cylindrical, which was not conducive to mixed application with other fertilizers and mechanized fertilization, and formaldehyde was added in the production process, which may pose a threat to human and environmental health (Wang et al., 2023). UPU and UPUM fertilizer granules deform at 80 °C and 100 °C respectively. Owing to the presence of UP and U, the characteristic peak (P-O-P) of polyphosphates was observed in the infrared spectra of UPU (895 cm^{-1}) and UPUM (911 cm^{-1}). The peaks of the P-O-P bond in UPUM and UPUKM shifted to higher wavenumbers than those in UPU, which may be due to the hydrogen bonds between polyphosphate and montmorillonite.

The higher deformation temperature of UPUM than that of UPU could be attributed to the layered structure of montmorillonite in UPUM, which slows down the contact and reaction between urea phosphate and urea. On the other hand, it may be that potassium ions in the inter-layer space of montmorillonite in UPUKM might have been strongly adsorbed by the negative charges of the two adjacent layers, rendering montmorillonite a much more stable structure, slowing down the contact and reaction between urea phosphate and urea, and keeping the fertilizer particles spherical (Morrow et al., 2013). Simultaneously, TGA analysis was performed on different treatments of fertilizers, revealing a trend in thermal stability following the sequence UPUKM > UPUM > UPU. This trend was consistent with the observed phenomena during the reaction process and further showed that the addition of nanoscale montmorillonite could enhance the stability of the fertilizer. The addition of potassium chloride further improved the thermal stability of the fertilizers (Fig. S2). The characteristic peaks at 3457, 3364, 3427, and 3333 cm^{-1} in the FTIR spectrum are attributed to the stretching vibration of –NH in urea phosphate and urea in FTIR (Fig. 1c). The peaks at 1034, 1038, and 1029 cm^{-1} are related to Si-O-Si in montmorillonite. The peaks at 1080 and 1066 cm^{-1} are due to the stretching vibration of P-O. The peaks at 1012 and 1003 cm^{-1} correspond to the symmetrical stretching vibration of PO_2.

3.2. XRD analysis of prepared fertilizer

XRD is commonly employed to determine the interlayer spacing between minerals and nanocomposites (Vo et al., 2019; Zhang et al., 2020). The larger basal spacing in UM (d = 1.81) than that in montmorillonite may be due to the entry of urea into the interlayer of M (d = 1.27) (Fig. 2). The basal spacing of UPM was the same as that of the montmorillonite, but the reflection was weaker because of the partial destruction of the layered structure of the montmorillonite (Yadav and Asthana, 2002; Pacuła et al., 2014). UP, U, K and UPU had no characteristic diffraction peak in the range of $2\theta = 3 \sim 10°$. The interlayer spacings of KM was 1.15 nm. This distance may be because potassium ions enter the montmorillonite lattices, strengthening the bonding of adjacent crystal layers and, thus, reducing interlayer spacing (Jiang et al., 2014; Moslemizadeh et al., 2019). The interlayer spacing of UPUM and UPUKM was 1.43 nm and 1.41 nm, respectively. The difference in the trend of interlayer spacing between UPUKM and UPUM may be attributed to the fixation of montmorillonite by potassium in UPUKM, which reduced the interlayer spacing of montmorillonite as discussed in previous sections (Huang et al., 2018; Wang 2020). Overall, the interlayer spacings of UPUM and UPUKM were larger than those of the original montmorillonite, indicating the formation of polyphosphate-montmorillonite nanocomposites in both UPUM and UPUKM.

3.3. Morphology analysis of prepared fertilizer

Further investigation of the nanostructure was performed using field emission scanning electron microscopy (SEM) and transmission electron microscopy (TEM). As shown in Fig. 3, the raw MMT clay exhibited a thin, flexible plate-like morphology (Fig. 3a1). However, in UPUKM, urea phosphate reacted with urea to form chain polyphosphate, and montmorillonite was dispersed in the polymer in the fertilizer (Fig. 3b1). Additional, structural information was obtained from the TEM micrographs of the as-prepared samples. An ordered crystal layer structure of montmorillonite was observed. In UPUKM, the silicate layer of montmorillonite was dispersed in the fertilizer particles, but the interlayer structure became disordered and exfoliated. The polyphosphate/-montmorillonite nanocomposites with an exfoliated structure were more beneficial to the mechanical properties. The mechanical properties of the nanocomposites are improved due to the strong interaction between the nanoparticles and the polymer matrix and the reduction of the distance between the particles (Xie et al., 2022).

3.4. Optimum UPUKM preparation process

The UPUKM preparation process was analyzed using ANOVA to identify the effect of the raw material mass ratio on the angle of repose (Y_1) and hardness (Y_2) of the fertilizer (Table 4). Two polynomial models with statistical significance were generated using a combination of the parameter estimates.

$$Y_1 = 46.50 + 21.63A - 6.45B - 7.48AB \quad (2)$$

$$Y_2 = 31.51 - 0.9466A - 1.61B - 0.7739AB + 0.1496A^2 + 0.6075B^2 \quad (3)$$

The regression equations were significant ($p < 0.0001$), the lack of fit was not significant ($P > 0.05$), and R^2 and Adj R^2 were > 90% (Table 4), indicating that the models could explain most of the changes in the response variables.

The obtained surface obtained based on the quadratic models are presented in Fig. 5. When the mass of potassium chloride was constant, the particle hardness of the fertilizer increased, and the fluidity gradually decreased with an increase in the mass of urea phosphate. This finding was expected because with more polyphosphate generated due to the increase of urea phosphate, the particle hardness of the fertilizer increased. Simultaneously, with an increase in urea phosphate, as discussed previously, the reaction between urea phosphate and urea increases in intensity, and the fertilizer system becomes unstable, resulting in the deformation of fertilizer particles and an increase in the angle of repose or a decrease in particle fluidity. The optimal raw material mass ratio was found to be 1:1:0.93:1 (urea phosphate: urea: potassium chloride: montmorillonite), at which point the particle fluidity and hardness of the prepared fertilizer were maximized (see Table 5).

The effects of reaction temperature (C) and reaction time (D) on the hardness and angle of repose of the fertilizer particles are expressed by Eqs. (4) and (5):

$$Y_1 = 60.16 + 4.76C + 16.47D - 3.87CD - 9.14C^2 - 20.99D^2 \quad (4)$$

$$Y_2 = 31.22 - 0.5299C + 0.1019D + 0.3250CD + 0.5140C^2 + 3.69D^2 \quad (5)$$

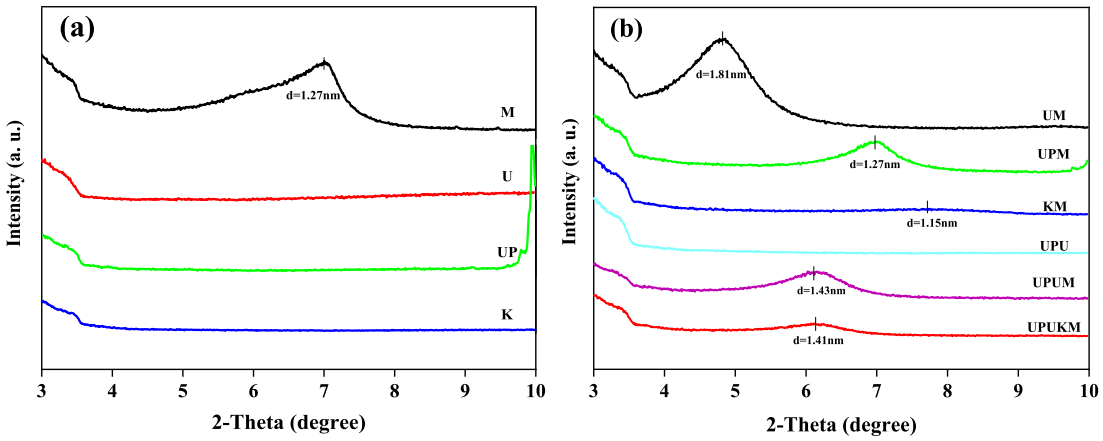

Fig. 2 XRD patterns of the raw materials (a) and the prepared fertilizers (b). d-spacing was calculated from the Bragg Law: $2d\sin\theta = n\lambda$. See Table 1 for details of the fertilizers.

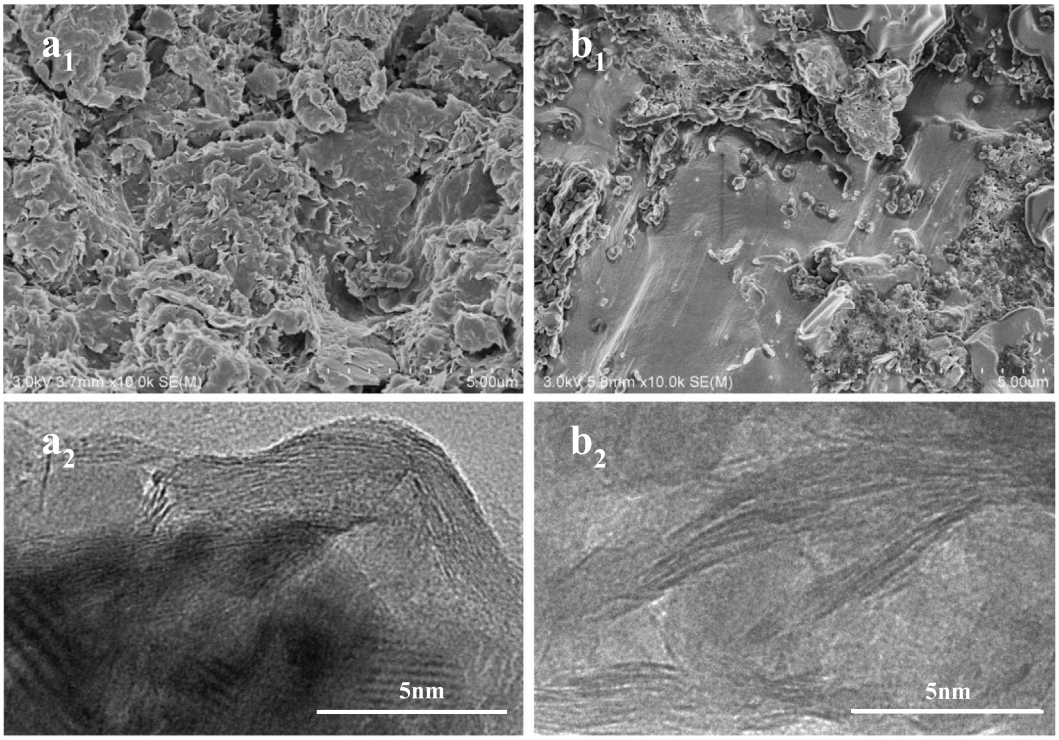

Fig. 3 The SEM (a_1, b_1) and TEM (a_2, b_2) images of montmorillonite (a) and interior of UPUKM (b).

The response surfaces of the response variables are presented in Fig. 6. Temperature strongly influenced on the hardness and fluidity of the fertilizer particles. The hardness and fluidity of the fertilizer particles first increased and then decreased with increasing reaction temperature, indicating that when the reaction temperature was too high, the reaction between urea phosphate and urea was so violent that the fertilizer particles were deformed, the fertilizer angle of repose increased, and the fluidity decreased.

The optimum process conditions identified by response surface analysis (Figs. 4 and 5) were reaction temperature, 103 °C; reaction time, 237 min; and mass ratio, 1:1:0.93:1 (urea phosphate: urea: potassium chloride: montmorillonite). Under these optimum conditions, the particle hardness and angle of repose of the prepared fertilizer were 64.75 ± 0.48 N and 30.84 ± 0.95°, respectively, which were close to the software-predicted values of 62.54 N and 31.21°, respectively.

3.5. Nutrient release behavior of the prepared fertilizers

N, P, and K were rapidly released from the CCF in the first three cycles (Fig. 6). For CCF, 100% of total N, 93% of total P, and 100% of total K were released and leached from the column three times, with up to 68% N, 72% P, and 60% K

Table 4 ANOVAs for regression models between particle angle of repose (Y_1)/particle hardness (Y_2) and the masses of the two raw materials of urea phosphate (A) and potassium chloride (B).

Source[a]		Sum of squares	Df.	Mean square	F-value	P-value	Significance[b]
Model	Y_1	5765.25	5	1153.05	41.02	< 0.0001	**
	Y_2	4322.77	3	1440.92	75.93	< 0.0001	**
A	Y_1	3744.34	1	3744.34	197.30	< 0.0001	**
	Y_2	7.17	1	7.17	52.36	0.0002	*
B	Y_1	332.56	1	332.56	17.52	0.0024	*
	Y_2	20.82	1	20.82	152.07	< 0.0001	**
AB	Y_1	245.86	1	245.86	12.96	0.0058	*
	Y_2	2.40	1	2.40	17.50	0.0041	*
A^2	Y_1	–	–	–	–	–	
	Y_2	0.1557	1	0.1557	1.14	0.3217	
B^2	Y_1	–	–	–	–	–	
	Y_2	2.57	1	2.57	18.75	0.0034	*
Residual	Y_1	170.80	9	18.98	–	–	
	Y_2	0.9585	7	0.1369			
Lack of fit	Y_1	145.51	5	29.10	4.60	0.0821	Not significant
	Y_2	0.6678	3	0.2226	3.06	0.1539	Not significant
Pure error	Y_1	25.29	4	6.32			
	Y_2	0.2907	4	0.0727			
Corr. total	Y_1	4493.57	12				
	Y_2	33.95	12				

Y_1: $R^2 = 0.9620$, Adj $R^2 = 0.9493$; Y_2: $R^2 = 0.9718$, Adj $R^2 = 0.9516$.

b*Significant at $p < 0.05$, **Significant at $p < 0.01$.

Table 5 ANOVAs for regression models between particle angle of repose (Y_1)/particle hardness (Y_2) and reaction time (C, min) and reaction temperature (D, °C).

Source[a]		Sum of squares	Df.	Mean square	F-value	P-value	Significance[b]
Model	Y_1	5765.25	5	1153.05	41.02	< 0.0001	**
	Y_2	97.59	5	19.52	35.83	< 0.0001	**
A	Y_1	181.29	1	181.29	6.45	0.0387	
	Y_2	2.24	1	2.24	4.11	0.0822	
B	Y_1	2168.93	1	2168.93	77.15	< 0.0001	*
	Y_2	0.0831	1	0.0831	0.1525	0.7077	**
AB	Y_1	60.06	1	60.06	2.14	0.1872	*
	Y_2	0.4225	1	0.4225	0.7756	0.4077	*
A^2	Y_1	581.62	1	581.62	20.69	0.0026	
	Y_2	1.84	1	1.84	3.37	0.1088	
B^2	Y_1	3064.54	1	3064.54	109.01	< 0.0001	
	Y_2	94.84	1	94.84	174.11	< 0.0001	*
Residual	Y_1	196.79	7	28.11			
	Y_2	3.81	7	0.5447			
Lack of fit	Y_1	160.78	3	53.59	5.95	0.0588	Not significant
	Y_2	3.17	3	1.06	6.55	0.0506	Not significant
Pure error	Y_1	36.01	4	9.00			
	Y_2	0.6453	4	0.1613			
Corr. total	Y_1	5962.04	12				
	Y_2	101.41	12				

Y_1: $R^2 = 0.9670$, Adj $R^2 = 0.9434$; Y_2: $R^2 = 0.9624$, Adj $R^2 = 0.9355$.

b*Significant at $p < 0.05$, **Significant at $p < 0.01$.

leached the first time. P was released and leached from the column five times.

Nutrient release from UPUKM was much slower: 11.60%–15.67% and 33.59%–55.59% of the three nutrients were released and leached from the column in the first and second cycles, respectively. After five leaching cycles, nutrient release from UPUKM became even slower than that aforementioned, and after 12 leaching cycles, approximately 92%-94% of the three nutrients were released. Because UP and urea enter the interlayer of montmorillonite, polyphosphates are formed via in situ polymerization. Nutrients in the fertilizer were hindered by the interlayer of montmorillonite, which reduced nutrient

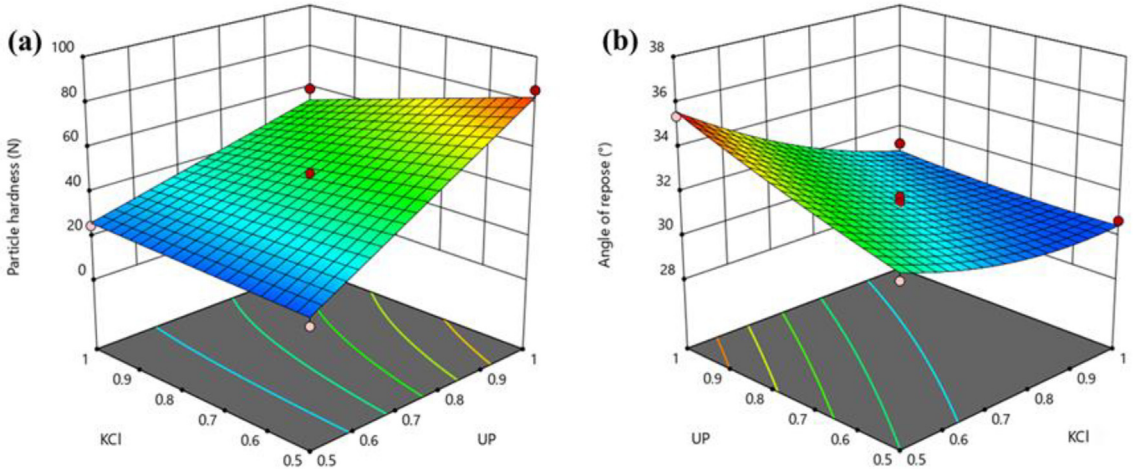

Fig. 4 Response surface plots showing effects of raw material mass ratio on particle hardness (a) and angle of repose (b) of prepared fertilizer. The two raw materials are urea phosphate (UP) and potassium chloride (KCl).

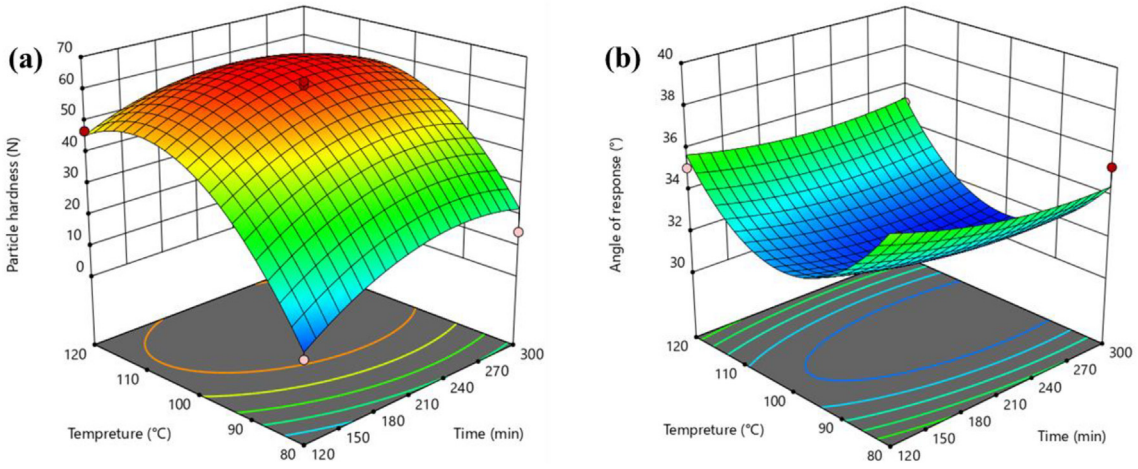

Fig. 5 Response surface plots showing effects of reaction temperature and time on particle hardness (a) and angle of repose (b) of the prepared fertilizer.

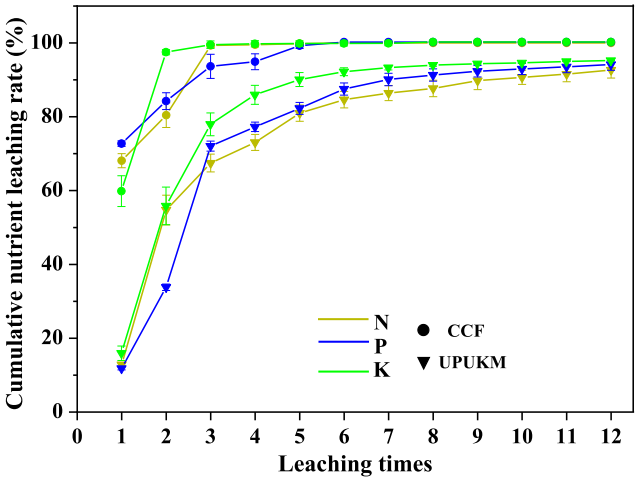

Fig. 6 Cumulative release of nitrogen (a), phosphorus (b), and potassium (c) from prepared fertilizers. CCF is a conventional chemical fertilizer with N-P_2O_5-K_2O of 21–14-20. See Table 1 for details of UPUK and UPUKM.

leaching. The slow release of potassium from UPUKM may be because the potassium ions were fixed in the montmorillonite lattice, forming a structure similar to that of mica, which can be used as a slow-release potash fertilizer (Said et al., 2018).

3.6. Fertilizer particle structures observed with XCT

To investigate the effect of urea phosphate and urea heating on the internal structure of fertilizer and the slow-release mechanism of fertilizer, UM, UPUKM, and eluted UPUKM fertilizer samples were scanned using XCT. XCT is a nondestructive method of scanning the internal structure so that the difference between each sample can be observed intuitively. X-ray computed tomography showed a clear core–shell structure in UM (Fig. 7a2$_3$), which is a characteristic of agglomeration and granulation products. The instability of this core–shell structure results in its lower particle strength, which was consistent with the particle strength of UM in Fig. 1, which was only 10.2 N. There was no core–shell structure in UPUKM, and the structure was uniform (Fig. 7b2),

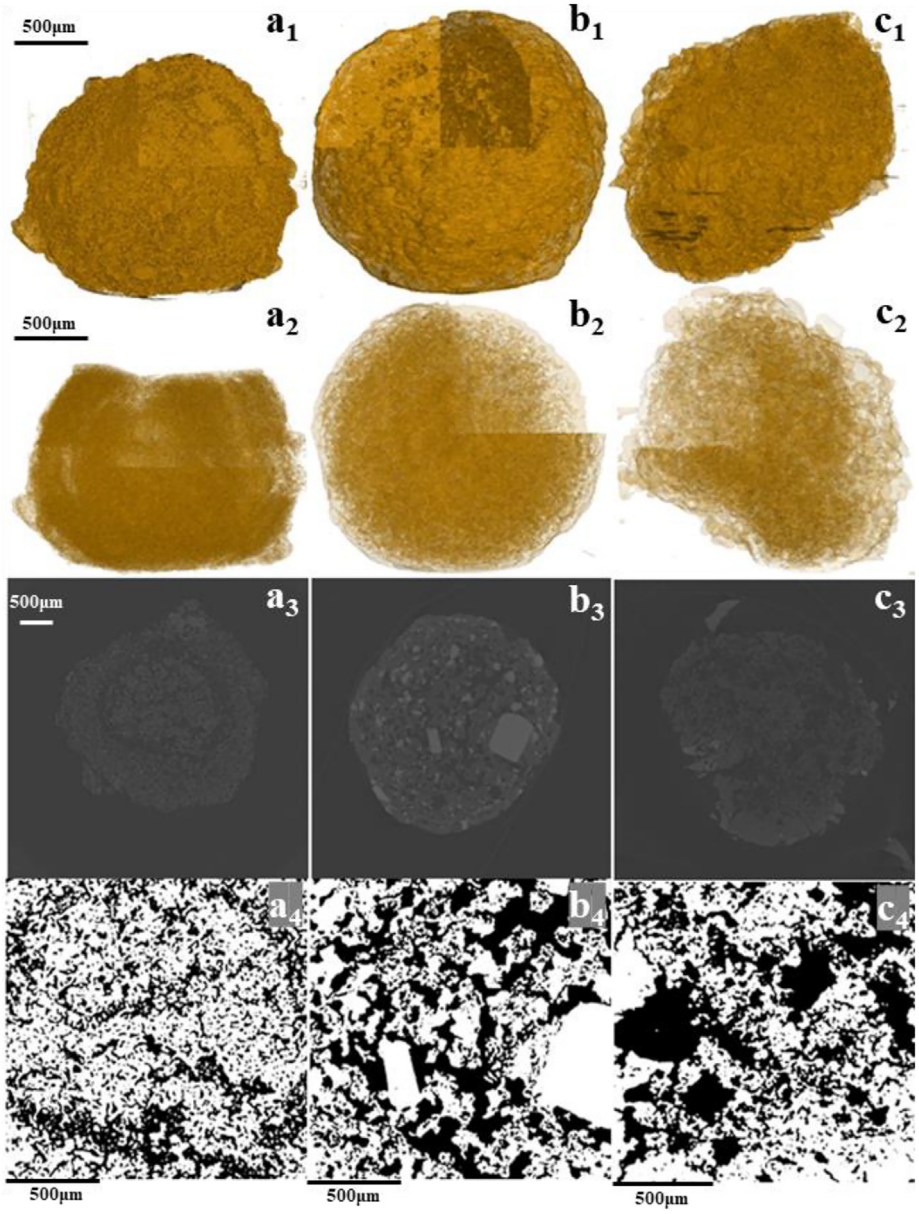

Fig. 7 X-ray microtomography images of UM (a), UPUKM (b), and UPUKM after the leaching experiment (c): (1), (2) reconstructed 3D images, (3) 2D slice images, (4) magnified 2D slice images. See Table 1 for details of the fertilizers.

with larger pores (Fig. 7b3,4). This may be the result of the reaction of urea phosphate and urea to form long-chain polyphosphate, and simultaneously the polyphosphate enters the interlayer of montmorillonite and exfoliated its nanosheets to form an interlocking structure, causing the core–shell structure to disappear and the particle strength to increase (Zhu et al., 2019). The addition of nano-materials makes the matrix and nanoparticles maintain uniform dispersion and good adhesion, and significantly increases the mechanical properties of the composite (Domun et al., 2015; Heidari et al., 2021; Garg et al., 2022). The research showed that carbon nanotube reinforced polymeric composite doubly curved micro-shell panels (Huang et al., 2021). This has a good inspiration for our future work, for example, we can explore the effect of different nano-materials on the strength of fertilizer particles. After the leaching experiment, larger pores are visible on the montmorillonite skeleton of UPUKM (Fig. 7c4), which may have been left behind after the soluble matter was leached out. The montmorillonite skeleton still exists after UPUKM has been completely eluted (Fig. 7c1), indicating that the stability of the fertilizer in the soil was relatively high. Furthermore, the structure of the montmorillonite skeleton also hinders the diffusion of nutrients, thereby slowing down the release of nutrients in the fertilizer.

3.7. Agronomic effectiveness of prepared fertilizer

The yield, plant height, and stem diameter of maize at the 12-leaf stage were 24.27%, 3.98%, and 10.13%, respectively, and were significantly higher in the UPUKM treatment than in the

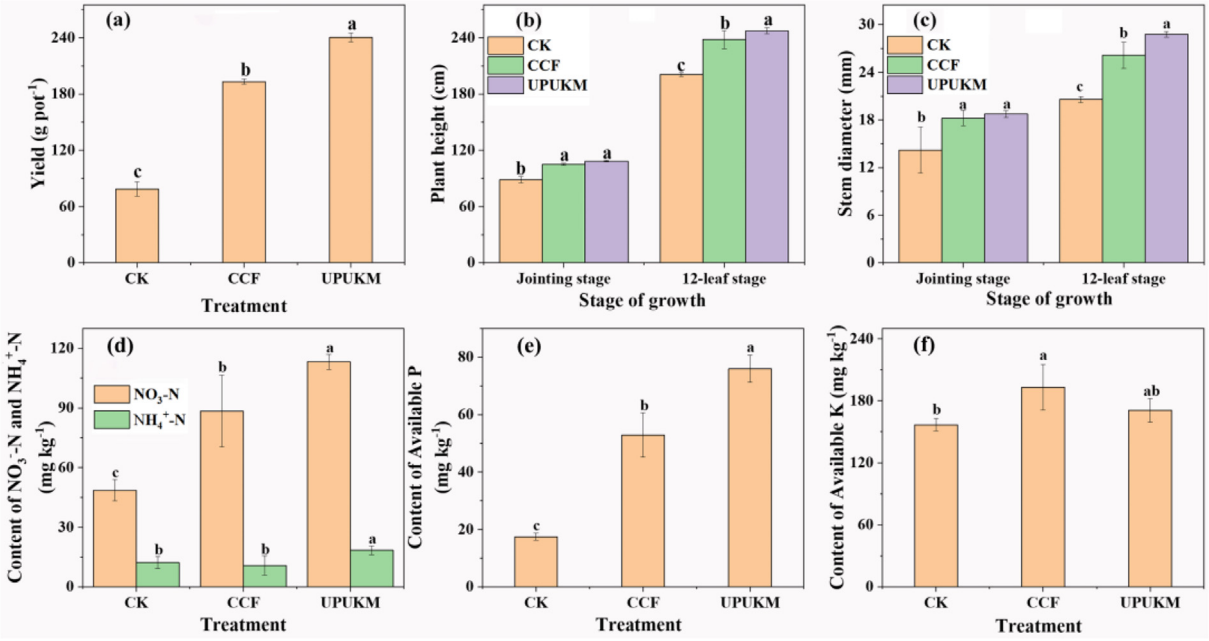

Fig. 8 Yield (a), plant height (b), stem diameter (c), available N (d), P (e), and K (f) at the jointing stage of maize in CK, CCF, and UPUKM. Soil of maize in CK, CCF, and UPUKM. Different letters above the bars indicate significant differences between the means by Duncan's multiple range test ($p < 0.05$, $n = 3$). CK: without fertilizer; CCF: conventional chemical fertilizer with N-P_2O_5-K_2O of 21–14-20. See Table 1 for details of UPUKM (N-P_2O_5-K_2O of 14–11-16).

CCF treatment (Fig. 8). This finding demonstrates that the slow release and sustained supply of nutrients from the prepared composite fertilizer (UPUKM) was the key to increasing the crop yield.

At the jointing stage of maize, the soil nitrate nitrogen content in UPUKM was 28.02%, significantly higher than that in CCF, and available phosphorus was significantly higher (43.45%) (Fig. 8). Maize is a fast-growing crop that requires a high level of phosphorus at the beginning of its life cycle. In this study, the UPUKM treatment significantly increased the soil available phosphorus content and promoted the absorption and utilization of phosphorus by maize. There was no significant difference in the soil available potassium content between treatments. Therefore, the UPUKM in the formula could be used as a nanocomposite to slow the release of nutrient elements, prepare a good nutrient resource and thus improve the crop yield (Salimi et al., 2021).

4. Conclusion

Because of the socioenvironmental problems caused by the highly soluble fertilizers currently used in agriculture, the development of new environmentally friendly products is extremely important for improving nutrient management. This study showed that the agglomeration granulation heating method was an effective way to prepare spherical nanocomposite slow-release fertilizer using urea phosphate, urea, potassium chloride and montmorillonite as raw materials. The formation of polyphosphate and its crosslinking with montmorillonite significantly enhances the particle strength of the fertilizers. The increase in interlayer spacing of montmorillonite and the exfoliation of its nanoplatelets, forming polyphosphate/montmorillonite nanocomposites, were confirmed by FT-IR, XRD, and TEM analyses. The optimal process parameters for preparing the fertilizer were obtained using the RSM-CCD method: reaction temperature, 103 °C; reaction time, 237 min; and mass ratio, 1:1:0.93:1 (urea phosphate: urea: potassium chloride: montmorillonite). Under these conditions, the fertilizer particles exhibit good physical properties with a hardness and angle of repose of 64.75 ± 0.48 N and 30.84 ± 0.95°, respectively. Leaching column experiments and XCT analysis demonstrated that the slow nutrient release was due to the nanocomposite structure. Pot experiments showed that the spherical polyphosphate/montmorillonite nanocomposite slow release fertilizer has the potential to improve soil nutrient supply and crop yield. This study provides a feasible method for the large-scale mechanized application of nanocomposite materials in agricultural fertilizers.

Acknowledgment

This study was supported by the National Natural Science Foundation of China (No. 42277356), and Major Basic research Project of Natural Science Foundation of Shandong Province (ZR202010200053-2), and Excellent Postdoctoral Program of Jiangsu Province in China (JB 0206025), and the National Key Research and Development Projects of China (2021YFD1700803-01-05).

Appendix A. Supplementary data

Supplementary data to this article can be found online at https://doi.org/10.1016/j.arabjc.2023.104871.

References

Albadarin, A.B., Lewis, T.D., Walker, G.M., 2017. Granulated polyhalite fertilizer caking propensity. Powder. Technol. 308, 193–199. https://doi.org/10.1016/j.powtec.2016.12.004.

An, D., Liu, B., Yang, L., Wang, T.J., Kan, C., 2017. Fabrication of graphene oxide/polymer latex composite film coated on KNO_3

fertilizer to extend its release duration. Chem. Eng. J. 311, 318–325. https://doi.org/10.1016/j.cej.2016.11.109.

Asimakopoulou, E., Zhang, J., Mckee, M., Wieczorek, K., Krawczyk, A., Andolfo, M., Kozlecki, T., Scatto, M., Sisani, M., Bastianini, M., 2020. Effect of layered double hydroxide, expanded graphite and ammonium polyphosphate additives on thermal stability and fire performance of polyisocyanurate insulation foam. Thermochim. Acta. 693,. https://doi.org/10.1016/j.tca.2020.178724 178724.

Bhat, A.H., Rangreez, T.A., Chisti, H.-T.-N., 2022. Wastewater treatment and biomedical applications of montmorillonite based nanocomposites: a review. Curr. Anal. Chem. 18, 269–287. https://doi.org/10.2174/1573411016999200729123309.

Borges, R., Baika, L.M., Grassi, M.T., Wypych, F., 2018. Mechanochemical conversion of chrysotile/K_2HPO_4 mixtures into potential sustainable and environmentally friendly slow-release fertilizers. J. Environ. Manage. 206, 962–970. https://doi.org/10.1016/j.jenvman.2017.11.082.

Chai, X., Chen, L., Xue, B., Liu, E., 2017. Granulation of ammonium chloride fertilizer and agglomeration mechanism. Powder. Technol. 319, 148–153. https://doi.org/10.1016/j.powtec.2017.06.045.

Chelladurai, S.J.S., Murugan, K., Ray, A.P., Upadhyaya, M., Narasimharaj, V., Gnanasekaran, S., 2021. Optimization of process parameters using response surface methodology: A review. Mater. Today: Proc. 37, 1301–1304. https://doi.org/10.1016/j.matpr.2020.06.466.

Cichy, B., Folek, S., 2005. Utilization of complexing abilities of polyphosphates in liquid fertilizers, based on the example of fertilizer type NP and type NPK with zinc. Ind. Eng. Chem. Res. 44, 4513–4517. https://doi.org/10.1021/ie049541d.

Danmaliki, G.I., Saleh, T.A., Shamsuddeen, A.A., 2017. Response surface methodology optimization of adsorptive desulfurization on nickel/activated carbon. Chem. Eng. J. 313, 993–1003. https://doi.org/10.1016/j.cej.2016.10.141.

De Simone, V., Caccavo, D., Lamberti, G., d'Amore, M., Barba, A.A., 2018. Wet-granulation process: phenomenological analysis and process parameters optimization. Powder. Technol. 340, 411–419. https://doi.org/10.1016/j.powtec.2018.09.053.

Degrève, J., Baeyens, J., Van de Velden, M., De Laet, S., 2006. Spray-agglomeration of NPK-fertilizer in a rotating drum granulator. Powder. Technol. 163, 188–195. https://doi.org/10.1016/j.powtec.2006.01.019.

Domun, N., Hadavinia, H., Zhang, T., Sainsbury, T., Liaghat, G., Vahid, S., 2015. Improving the fracture toughness and the strength of epoxy using nanomaterials-a review of the current status. Nanoscale. 7, 10294–10329. https://doi.org/10.1039/c5nr01354b.

Dubey, A., Mailapalli, D.R., 2019. Zeolite coated urea fertilizer using different binders: Fabrication, material properties and nitrogen release studies. Environ. Technol. Inno. 16,. https://doi.org/10.1016/j.eti.2019.100452 100452.

Dziadkowiec, J., Mansa, R., Quintela, A., Rocha, F., Detellier, C., 2017. Preparation, characterization and application in controlled release of ibuprofen-loaded guar gum/montmorillonite bio-nanocomposites. Appl. Clay. Sci. 135, 52–63. https://doi.org/10.1016/j.clay.2016.09.003.

Ferreira, I., Peruchi, R., Fernandes, N., Junior, P.R., 2021. Measurement system analysis in angle of repose of fertilizers with distinct granulometries. Measurement. 170,. https://doi.org/10.1016/j.measurement.2020.108681 108681.

Garg, A., Aggarwal, P., Aggarwal, Y., Belarbi, M., Chalak, H., Tounsi, A., Gulia, R., 2022. Machine learning models for predicting the compressive strength of concrete containing nano silica. Comput. Concrete. 30, 33–42 http://doi.org/10.12989/cac.2022.30.1.033.

Golbashy, M., Sabahi, H., Allahdadi, I., Nazokdast, H., Hosseini, M., 2017. Synthesis of highly intercalated urea-clay nanocomposite via domestic montmorillonite as eco-friendly slow-release fertilizer. Arch. Agron Soil Sci. 63, 84–95. https://doi.org/10.1080/03650340.2016.1177175.

Gong, W., 2001. A real time in situ ATR-FTIR spectroscopic study of linear phosphate adsorption on titania surfaces. Int. J. Miner process. 63, 147–165. https://doi.org/10.1016/S0301-7516(01)00045-X.

Guha, T., Gopal, G., Kundu, R., Kundu, R., Mukherjee, A., 2020. Nanocomposites for delivering agrochemicals: A comprehensive review. J. Agric. Food Chem. 68 (12), 3691–3702. https://doi.org/10.1021/acs.jafc.9b06982.

Guo, Y., Liu, Z., Zhang, M., Tian, X., Chen, J., Sun, L., 2018. Synthesis and application of urea-formaldehyde for manufacturing a controlled-release potassium fertilizer. Ind. Eng. Chem. Res. 57, 1593–1606. https://doi.org/10.1021/acs.iecr.7b04629.

Heidari, E., Sobati, M.A., Movahedirad, S., 2020. Dynamics of particle wetting in wet granulation: Micro-scale analysis. Int. J. Heat Mass Tran. 146,. https://doi.org/10.1016/j.ijheatmasstransfer.2019.118853 118853.

Heidari, F., Taheri, K., Sheybani, M., Janghorban, M., Tounsi, A., 2021. On the mechanics of nanocomposites reinforced by wavy/defected/aggregated nanotubes. Steel & Compos Struct: An. Int. J. 38 http://doi.org/10.12989/scs.2021.38.5.533.

Hodge, C.A., Motes, T., 1994. Production of high-quality liquid fertilizers from wet-process acid via urea phosphate. Fertil. Res. 39, 59–69. https://doi.org/10.1007/BF00750157.

Huang, Y., Karami, B., Shahsavari, D., Tounsi, A., 2021. Static stability analysis of carbon nanotube reinforced polymeric composite doubly curved micro-shell panels. Arch. Civ. Mech. Eng. 21, 139. https://doi.org/10.1007/s43452-021-00291-7.

Huang, X., Shen, H., Sun, J., Lv, K., Liu, J., Dong, X., Luo, S., 2018. Nanoscale laponite as a potential shale inhibitor in water-based drilling fluid for stabilization of wellbore stability and mechanism study. ACS Appl. Mater. Interfaces. 10, 33252–33259. https://doi.org/10.1021/acsami.8b11419.

Idumah, C.I., Okonkwo, U., Obele, C., 2022. Recently emerging advancements in montmorillonite polymeric nanoarchitectures and applications. Clean. Mater. 100071. https://doi.org/10.1016/j.clema.2022.100071.

Jahangirian, H., Rafiee-Moghaddam, R., Jahangirian, N., Nikpey, B., Jahangirian, S., Bassous, N., Saleh, B., Kalantari, K., Webster, T. J., 2020. Green synthesis of zeolite/Fe_2O_3 nanocomposites: toxicity & cell proliferation assays and application as a smart iron nanofertilizer. Int. J. Nanomed. 1005–1020. https://doi.org/10.2147/IJN.S231679.

Jiang, G., Xuan, Y., Li, Y., Wang, J., 2014. Inhibitive effect of potassium methylsiliconate on hydration swelling of montmorillonite. Colloid J+. 76, 408–415. https://doi.org/10.7868/S0023291214040065.

Kabiri, S., Baird, R., Tran, D.N., Andelkovic, I., McLaughlin, M.J., Losic, D., 2018. Cogranulation of low rates of graphene and graphene oxide with macronutrient fertilizers remarkably improves their physical properties. ACS Sustainable Chem. Eng. 6, 1299–1309. https://doi.org/10.1021/acssuschemeng.7b03655.

Kabiri, S., Tran, D.N., Baird, R., McLaughlin, M.J., Losic, D., 2020. Revealing the dependence of graphene concentration and physicochemical properties on the crushing strength of co-granulated fertilizers by wet granulation process. Powder Technol. 360, 588–597. https://doi.org/10.1016/j.powtec.2019.10.047.

Kim, K.S., Park, M., Choi, C.L., Lee, D.H., Seo, Y.J., Kim, C.Y., Kim, J.S., Yun, S.-I., Ro, H.-M., Komarneni, S., 2011. Suppression of NH_3 and N_2O emissions by massive urea intercalation in montmorillonite. J. Soil. Sediment. 11, 416–422. https://doi.org/10.1007/s11368-010-0326-z.

Lewis, H.T., Jones, T.M., Burnell, J.R., 1983. Two-stage process for crystallization of urea phosphate for production of clear polyphosphate liquid fertilizer. Ind. Eng. Chem. Prod. Res. Dev. 22, 111–117. https://doi.org/10.1021/i300009a025.

Lim, K.S., Bee, S.T., Sin, L.T., Tee, T.T., Ratnam, C.T., Hui, D., Rahmat, A.R., 2016. A review of application of ammonium polyphosphate as intumescent flame retardant in thermoplastic composites. Compos. Part. B-Eng. 84, 155–174. https://doi.org/10.1016/j.compositesb.2015.08.066.

Madusanka, N., Sandaruwan, C., Kottegoda, N., Sirisena, D., Munaweera, I., De Alwis, A., Karunaratne, V., Amaratunga, G. A., 2017. Urea–hydroxyapatite-montmorillonite nanohybrid composites as slow release nitrogen compositions. Appl. Clay. Sci. 150, 303–308. https://doi.org/10.1016/j.clay.2017.09.039.

Mathur, M.A., Dias, M.F., Mathur, M.P., 2016. Importance of green technology in fertilizer quality improvement. Procedia Eng. 138, 308–313. https://doi.org/10.1016/j.proeng.2016.02.089.

Morrow, C.P., Yazaydin, A.O.Z.R., Krishnan, M., Bowers, G.M., Kalinichev, A.G., Kirkpatrick, R.J., 2013. Structure, energetics, and dynamics of smectite clay interlayer hydration: Molecular dynamics and metadynamics investigation of Na-hectorite. J. Phys. Chem. C. 117, 5172–5187. https://doi.org/10.1021/jp312286g.

Moslemizadeh, A., Samadzadeh Hafshejani, K., Shahbazi, K., Zaravi Dezfuli, M., Zendehboudi, S., 2019. A biosurfactant for inhibiting clay hydration in aqueous solutions: applications to petroleum industry. Can. J. Chem. Eng. 97, 384–394. https://doi.org/10.1002/cjce.23172.

Naraginti, S., Yu, Y.-Y., Fang, Z., Yong, Y.-C., 2019. Novel tetrahedral Ag_3PO_4@ N-rGO for photocatalytic detoxification of sulfamethoxazole: process optimization, transformation pathways and biotoxicity assessment. Chem. Eng. J. 375,. https://doi.org/10.1016/j.cej.2019.122035 122035.

Obraniak, A., Orczykowska, M., Olejnik, T.P., 2019. The effects of viscoelastic properties of the wetting liquid on the kinetics of the disc granulation process. Powder. Technol. 342, 328–334. https://doi.org/10.1016/j.powtec.2018.09.081.

Pacuła, A., Pamin, K., Zięba, A., Kryściak-Czerwenka, J., Olejniczak, Z., Serwicka, E.M., Drelinkiewicz, A., 2014. Physicochemical and catalytic properties of montmorillonites modified with 12-tungstophosphoric acid. Appl. Clay. Sci. 95, 220–231. https://doi.org/10.1016/j.clay.2014.04.016.

Pereira, E.I., Minussi, F.B., da Cruz, C.C., Bernardi, A.C., Ribeiro, C., 2012. Urea–montmorillonite-extruded nanocomposites: a novel slow-release material. J. Agric. Food. Chem. 60, 5267–5272. https://doi.org/10.1021/jf3001229.

Pereira, E.I.A., Nogueira, A.R., Cruz, C.C., Guimaraes, G.G., Foschini, M.M., Bernardi, A.C., Ribeiro, C., 2017. Controlled urea release employing nanocomposites increases the efficiency of nitrogen use by forage. ACS Sustainable Chem. Eng. 5, 9993–10001. https://doi.org/10.1021/acssuschemeng.7b01919.

Ren, Y., Zhai, Y., Wu, L., Zhou, W., Qin, H., Wang, P., 2021. Amine- and alcohol-functionalized ionic liquids: Inhibition difference and application in water-based drilling fluids for wellbore stability. Colloid. Surface. A. 609,. https://doi.org/10.1016/j.colsurfa.2020.125678 125678.

Ren, C., Zhang, X., Reis, S., Gu, B., 2022. Socioeconomic barriers of nitrogen management for agricultural and environmental sustainability. Agric. Ecosyst. Environ. 333,. https://doi.org/10.1016/j.agee.2022.107950 107950.

Said, A., Zhang, Q., Qu, J., Liu, Y., Lei, Z., Hu, H., Xu, Z., 2018. Mechanochemical activation of phlogopite to directly produce slow-release potassium fertilizer. Appl. Clay. Sci. 165, 77–81. https://doi.org/10.1016/j.clay.2018.08.006.

Salimi, M., Motamedi, E., Safari, M., Motesharezadeh, B., 2021. Synthesis of urea slow-release fertilizer using a novel starch-g-poly (styrene-co-butylacrylate) nanocomposite latex and its impact on a model crop production in greenhouse. J. Clean. Prod. 322,. https://doi.org/10.1016/j.jclepro.2021.129082 129082.

Sandomierski, M., Buchwald, Z., Voelkel, A., 2020. Calcium montmorillonite and montmorillonite with hydroxyapatite layer as fillers in dental composites with remineralizing potential. Appl. Clay. Sci. 198,. https://doi.org/10.1016/j.clay.2020.105822 105822.

Setshedi, K.Z., Bhaumik, M., Songwane, S., Onyango, M.S., Maity, A., 2013. Exfoliated polypyrrole-organically modified montmorillonite clay nanocomposite as a potential adsorbent for Cr (VI) removal. Chem. Eng. J. 222, 186–197. https://doi.org/10.1016/j.cej.2013.02.061.

Subero-Couroyer, C., Ghadiri, M., Brunard, N., Kolenda, F., 2005. Analysis of catalyst particle strength by impact testing: The effect of manufacturing process parameters on the particle strength. Powder. Technol. 160, 67–80. https://doi.org/10.1016/j.powtec.2005.08.005.

Tian, H., ZhiguangZhang, MinGuo, YanleZheng, LeiLi, Yuncong, C., 2019. Biobased polyurethane, epoxy resin, and polyolefin wax composite coating for controlled-release fertilizer. ACS Appl. Mater. Interfaces. 11. https://doi.org/10.1021/acsami.8b16030.

Vo, V.-S., Mahouche-Chergui, S., Nguyen, V.-H., Naili, S., Carbonnier, B., 2019. Crucial role of covalent surface functionalization of clay nanofillers on improvement of the mechanical properties of bioepoxy resin. ACS Sustainable Chem. Eng. 7, 15211–15220. https://doi.org/10.1021/acssuschemeng.9b02088.

Wang, L., 2020. Clay stabilization in sandstone reservoirs and the perspectives for shale reservoirs. Adv. Colloid Interfac. 276,. https://doi.org/10.1021/acssuschemeng.9b02088 102087.

Wang, S., Han, Q., Wei, Z., Wang, Y., Deng, L., Chen, M., 2023. Formaldehyde causes an increase in blood pressure by activating ACE/AT1R axis. Toxicology. 486,. https://doi.org/10.1016/j.tox.2023.153442 153442.

Wang, Y., Li, L., Han, S., Lei, B.-H., Abudoureheman, M., Yang, Z., Pan, S., 2017. Linear-to-λ-Shape P-O-P bond transmutation in polyphosphates with infinite $(PO_3)\infty$ chain. Inorg Chem. 56, 10139–10142. https://doi.org/10.1021/acs.inorgchem.7b01540.

Wang, X., Lü, S., Gao, C., Xu, X., Zhang, X., Bai, X., Liu, M., Wu, L., 2014. Highly efficient adsorption of ammonium onto palygorskite nanocomposite and evaluation of its recovery as a multifunctional slow-release fertilizer. Chem. Eng. J. 252, 404–414. https://doi.org/10.1016/j.cej.2014.04.097.

Washino, K., Tan, H., Hounslow, M., Salman, A., 2013. A new capillary force model implemented in micro-scale CFD-DEM coupling for wet granulation. Chem. Eng. Sci. 93, 197–205. https://doi.org/10.1016/j.ces.2013.02.006.

Xie, M., He, J., Li, X., Yang, R., 2022. Ammonium polyphosphate/montmorillonite nanocomposite with a completely exfoliated structure and charring-foaming agent flame retardant thermoplastic polyurethane. Mater. Sci. Eng: B. 283,. https://doi.org/10.1016/j.mseb.2022.115825 115825.

Xin, X., Qin, S., Zhang, J., Zhu, A., Yang, W., Zhang, X., 2017. Yield, phosphorus use efficiency and balance response to substituting long-term chemical fertilizer use with organic manure in a wheat-maize system. Field. Crop. Res. 208, 27–33. https://doi.org/10.1016/j.fcr.2017.03.011.

Yadav, G.D., Asthana, N.S., 2002. Kinetics and mechanism of selective monoacylation of mesitylene. Ind. Eng. Chem. Res. 41, 5565–5575. https://doi.org/10.1021/ie020152y.

Yahaya, S.M., Mahmud, A.A., Abdullahi, M., Haruna, A., 2022. Recent advances in the chemistry of N, P, K as fertilizer in soil-A review. Pedosphere. https://doi.org/10.1016/j.pedsph.2022.07.012.

Yamamoto, C.F., Pereira, E.I., Mattoso, L.H., Matsunaka, T., Ribeiro, C., 2016. Slow release fertilizers based on urea/urea-formaldehyde polymer nanocomposites. Chem. Eng. J. 287, 390–397. https://doi.org/10.1016/j.cej.2015.11.023.

Yang, L., Jiang, G., Shi, Y., Yang, X., 2017. Application of ionic liquid and polymeric ionic liquid as shale hydration inhibitors. Energy Fuels. 31, 4308–4317. https://doi.org/10.1021/acs.energyfuels.7b00272.

Yang, J., Kong, X., Xu, D., Xie, W., Wang, X., 2019. Evolution of the polydispersity of ammonium polyphosphate in a reactive extrusion process: Polycondensation mechanism and kinetics. Chem. Eng. J. 359, 1453–1462. https://doi.org/10.1016/j.cej.2018.11.031.

Zhang, H., Hodges, C.S., Mishra, P.K., Yoon, J.Y., Hunter, T.N., Lee, J.W., Harbottle, D., 2020a. Bio-inspired preparation of clay-hexacyanoferrate composite hydrogels as super adsorbents for Cs +. ACS Appl. Mater. Interfaces. 12, 33173–33185. https://doi.org/10.1021/acsami.0c06598.

Zhang, W., Xiang, Y., Fan, H., Wang, L., Xie, Y., Zhao, G., Liu, Y., 2020b. Biodegradable urea-formaldehyde/PBS and its ternary nanocomposite prepared by a novel and scalable reactive extrusion process for slow-release applications in agriculture. J. Agric. Food. Chem. 68, 4595–4606. https://doi.org/10.1021/acs.jafc.0c00638.

Zhou, L., Zhao, P., Chi, Y., Wang, D., Wang, P., Liu, N., Cai, D., Wu, Z., Zhong, N., 2017. Controlling the hydrolysis and loss of nitrogen fertilizer (urea) by using a nanocomposite favors plant growth. ChemSusChem. 10, 2068–2079. https://doi.org/10.1002/cssc.201700032.

Zhu, T.T., Zhou, C.H., Kabwe, F.B., Wu, Q.Q., Li, C.S., Zhang, J.R., 2019. Exfoliation of montmorillonite and related properties of clay/polymer nanocomposites. Appl. Clay. Sci. 169, 48–66. https://doi.org/10.1016/j.clay.2018.12.006.